


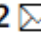
Literature Report

Reporter: zhou wei

Date: 2020-03-26



A DNA-based fluorescent probe maps NOS3 activity with subcellular spatial resolution

Maulik S. Jani^{1,2}, Junyi Zou^{1,2,3}, Aneesh T. Veetil^{1,2,3} and Yamuna Krishnan^{1,2}  



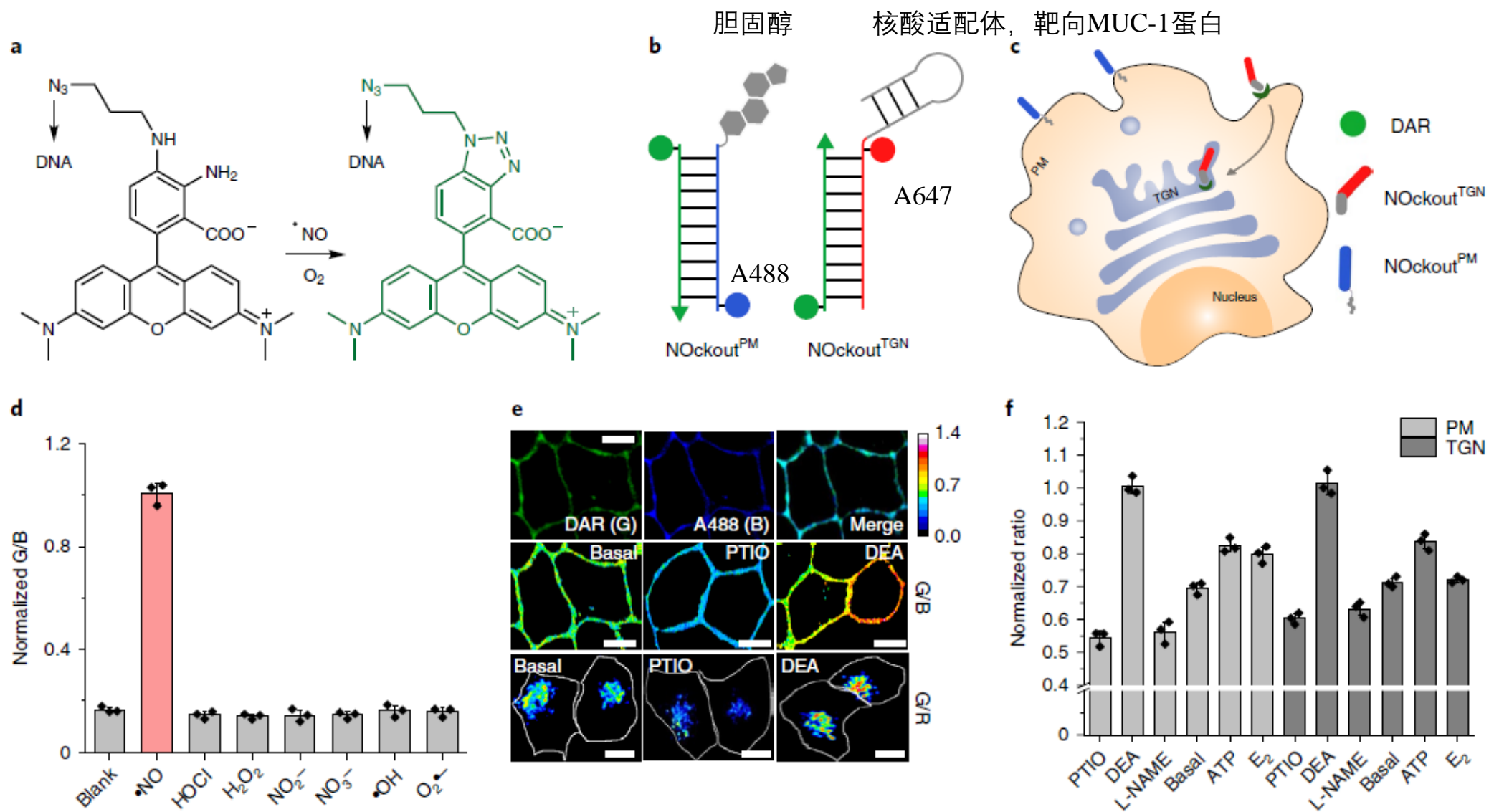
Professor, University of Chicago

Quantitative chemical imaging in living systems

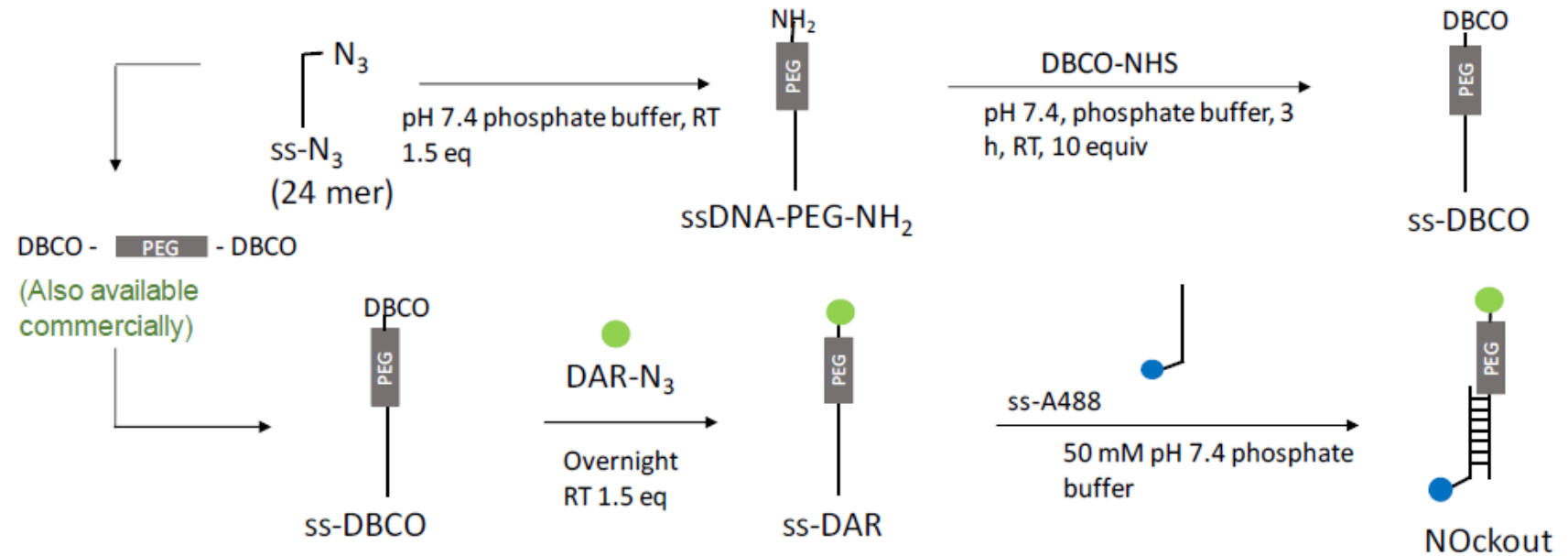
A: Quantitative, fluorescent chemical sensors

B: Cell-specific and organelle –specific targeting

C: Fundamental biology and biomedical applications

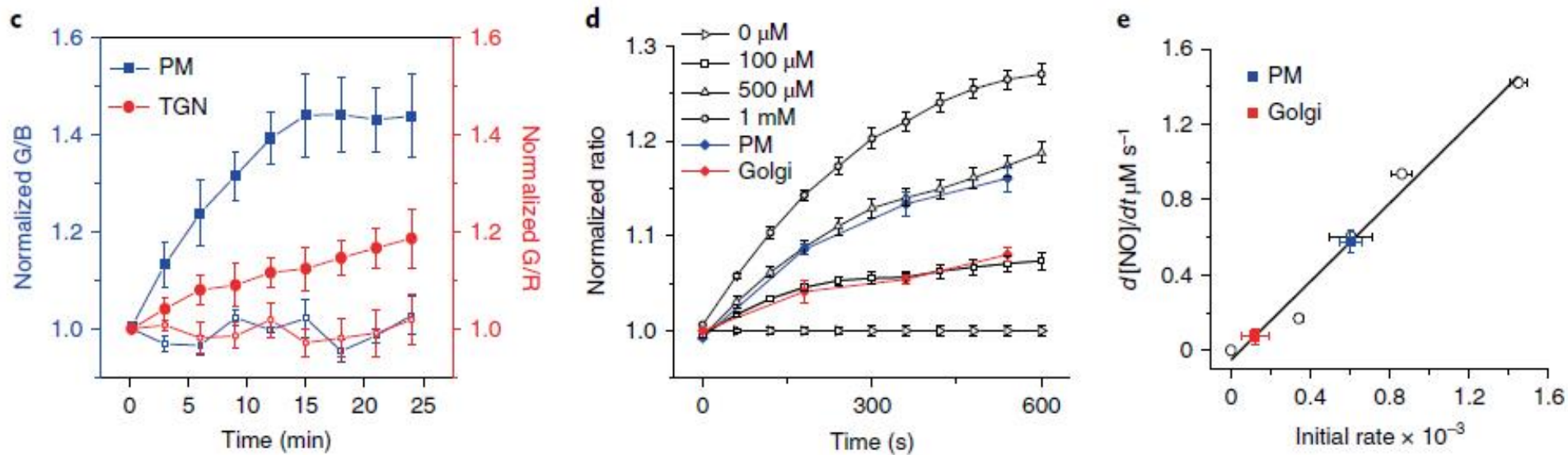
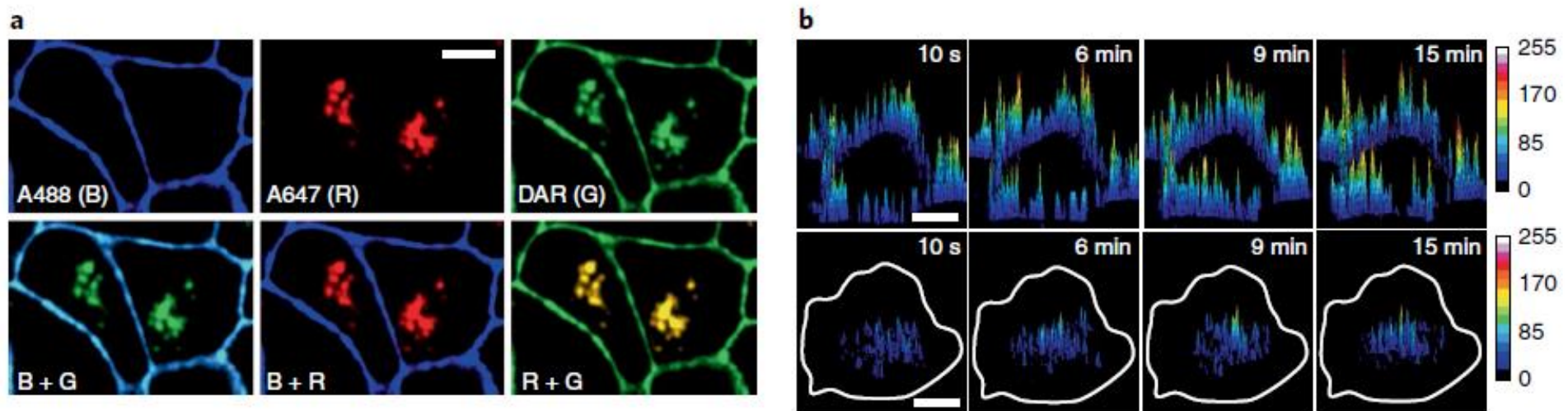


Name	Sequence
S1	5' - /5AzideN/ATC AAC ACT GCA CAC CAG ACA GCA -3'
S2 ^{PM}	5' - /5Alex488N/TGC TGT CTG GTG TGC AGT GTT GAT /3CholTEG/ -3'
S2 ^{TGN}	5' - GGC TAT AGC ACA TGG GTA AAA CGA CTT TGC T/iAlexa647N/G TCT GGT GTG CAG TGT TGA T -3'



Parameters	DAF-2DA ¹³ (commercial NO detection kits) (Fig S17)	G-geNOp ¹⁴ (protein sensor for NO) (Fig S18)	NOckout (this study)
Ratiometric	No (Fig. S17a)	No (Fig. S18a)	Yes (Fig. 1b-d and S1a-c)
Mode of sensing	Fluorescence turn on (Fig. S17a and c)	Fluorescence turn off (Fig. S18a and c)	Fluorescence turn on (Fig. S1b-c and S2a-b)
Sensitivity towards pH	Yes (Fig. S17b and d)	Yes (Fig. S18d-e)	No (Fig. S1d and S8e)
Cross-reactivity to H ₂ O ₂	None (Fig. S17e)	Yes (Fig. S18f)	None (Fig. 1d)
Fe ²⁺ supplementation	Not required (Fig. S17a and c)	Required (Fig. S18a-c)	Not required (Fig. S1b-c and S2a-b)
Maximum in-cellulo fold change	7500% (Fig. S17c)	-15% (Fig. S18c)	200% (Fig. 1f)
Organelle targetability	No (Fig. S17a)	Yes ¹⁴	Yes (Fig. S2c-d, S3 and S4)
Reversible	No ¹³	Quasi-reversible ¹⁴	No (Fig. S1b-c and S2a-b)

对于商业化的NO探针来说，综合性能较为优异，可以应用于细胞内的细胞器NO定量成像。



a, Simultaneous pulsing of NOckout_{PM} (500 nM) and NOckout_{TGN} (500 nM) on T-47D cells labels both plasma membrane and Golgi apparatus of the same cell. Representative images are shown from total of three independent experiments. **b**, NOckout_{PM} and NOckout_{TGN} report subcellular simultaneous NO dynamics on stimulation with thapsigargin (1 μM) in T-47D cells. Single confocal plane images were taken every 3 min for 24 min. NO signals are calculated as the ratio of DAR to A488 (in the case of NOckout_{PM}) and DAR to A647 (in the case of NOckout_{TGN}) to represent as surface plots using Fiji. Representative images are shown from total of three independent experiments. **c**, Kinetic traces of NO production from two distinct subcellular locations in live T-47D cells. Simultaneous NO signals from NOckout_{PM} and NOckout_{TGN} are monitored as a function of time from single cells, post thapsigargin treatment (filled squares and circles) or on PTIO treatment (empty squares and circles). Average intensities are plotted as ratios of DAR/A488 (G/B, NOckout_{PM}) and DAR/A647 (G/R, NOckout_{TGN}) for $n = 10$ cells. PM, plasma membrane. Error bars represent standard error of mean (s.e.m.) from three independent experiments. **d**, In cellulo kinetic traces showing G/B signal from NOckout_{PM} containing cells on treatment with indicated concentrations of DEA-NONOate, overlaid with NOckout_{PM} and NOckout_{TGN} traces from **c**. **e**, In vitro $(d[\text{NO}]/dt)$ versus in cellulo (initial rate $\times 10^{-3}$) graph overlaid with initial rates for thapsigargin (1 μM) treated plasma membrane (blue filled square) and Golgi (red filled square) calculated from (Supplementary Fig. 8c). Error bars represent standard error of mean (s.e.m.) from three independent experiments.

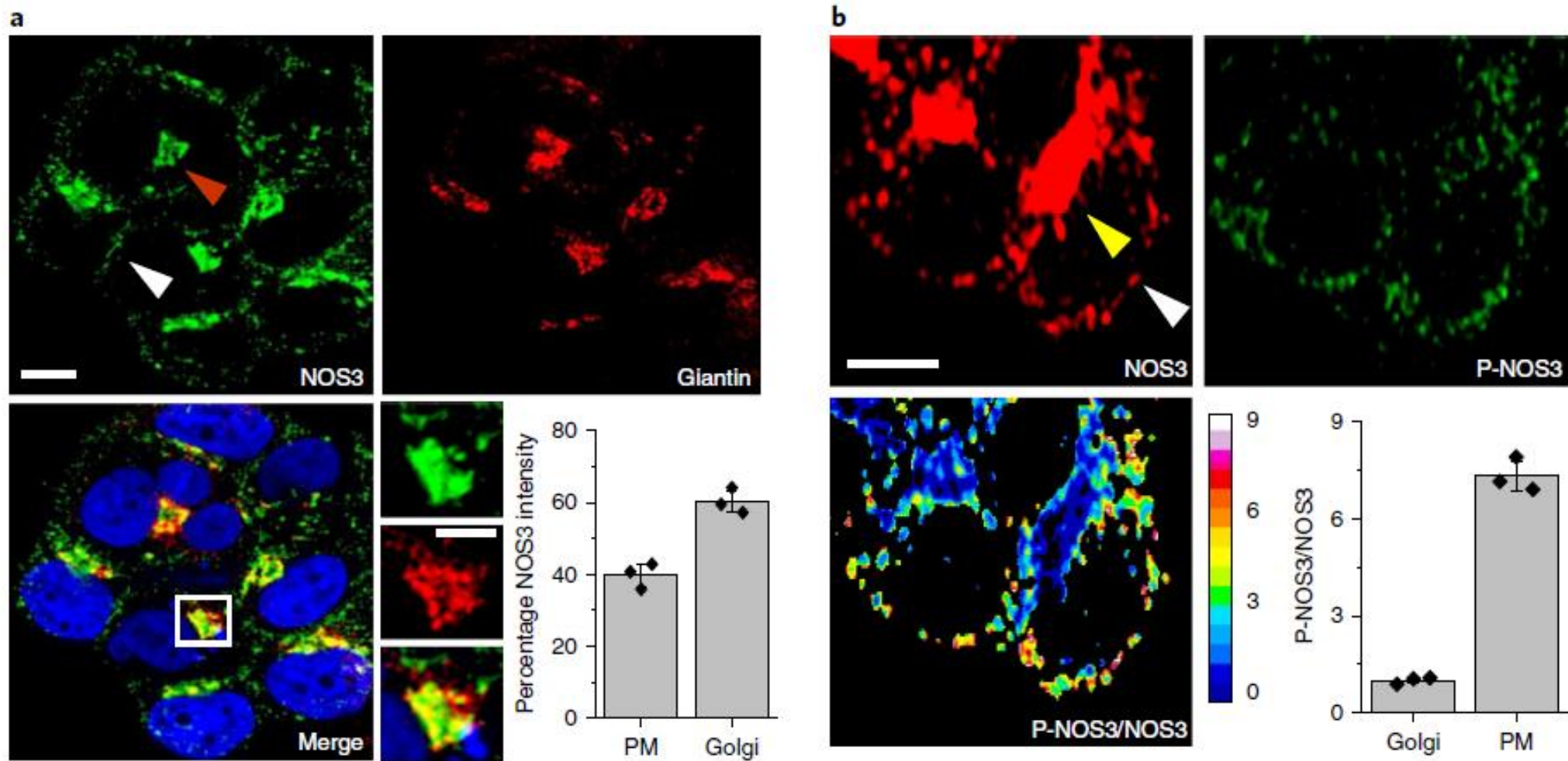


Fig. 3 | Phosphorylated NOS3 is enriched at the plasma membrane. **a**, Colocalization of NOS3 (green) with the Golgi marker protein Giantin (red) in T-47D cells. Inset shows merged images in higher magnification. White and maroon arrowheads represent NOS3 population at the plasma membrane (PM) and at the Golgi, respectively. Bar graphs show percentage of NOS3 located at the plasma membrane and at Golgi apparatus in T-47D cells. Error bars represent standard error of mean (s.e.m.) from three independent experiments, $n = 50$ cells. Scale bar, $10 \mu\text{m}$. **b**, Representative images of T-47D cells immunostained with **NOS3** and **P-NOS3** antibodies. Pseudo-colored P-NOS3/NOS3 image shows the extent of phosphorylation where white and yellow arrowheads represent NOS3 populations at the plasma membrane and at the Golgi, respectively. Quantification of the same is shown in the bar graph format. Error bars represent standard error of mean (s.e.m.) from three independent experiments, $n = 30$ cells. Scale bar, $10 \mu\text{m}$.

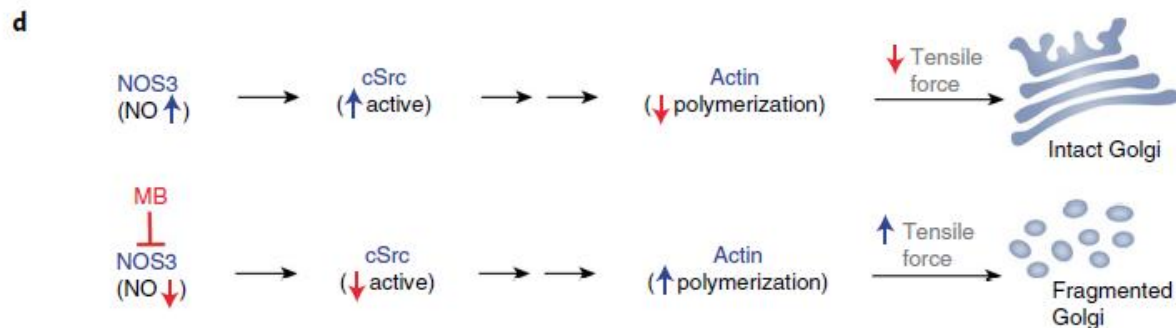
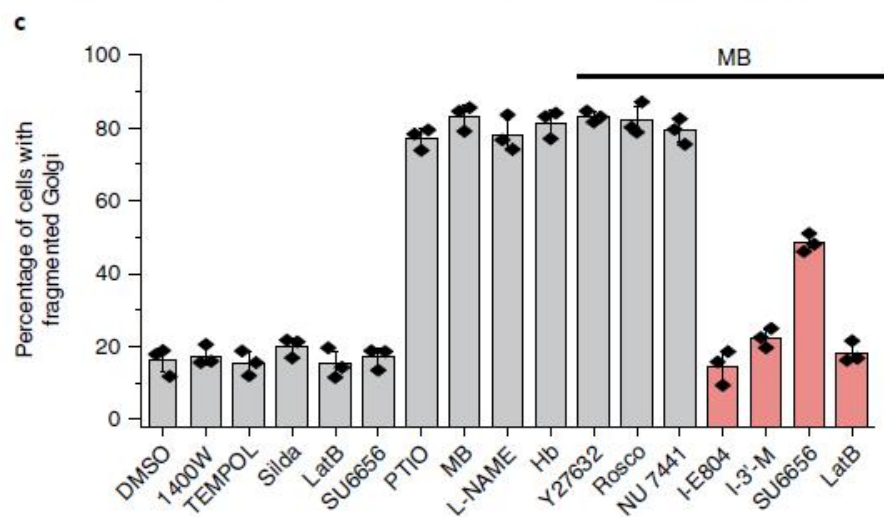
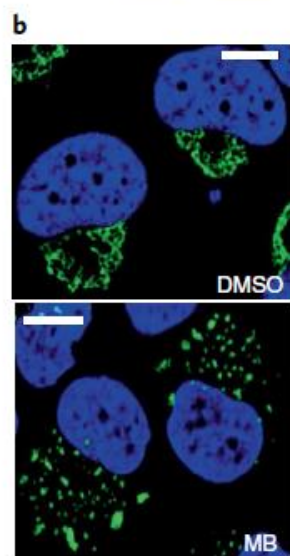
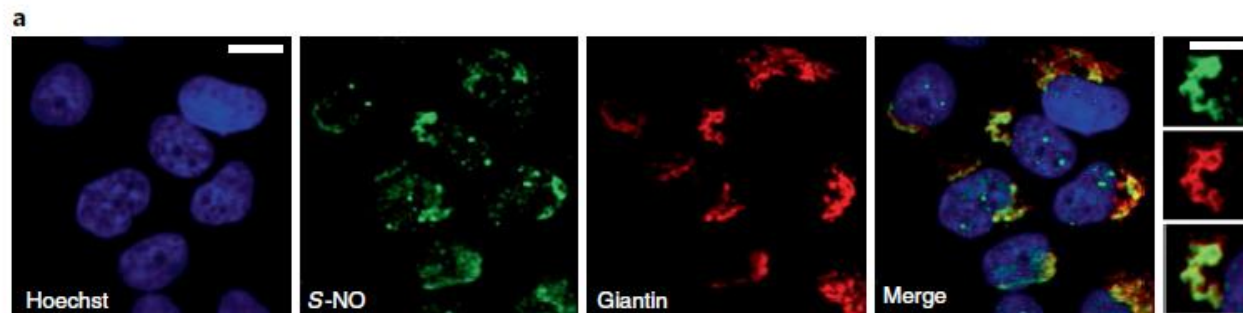


Fig. 4 | The Golgi is an *S*-nitrosylation hotspot in breast cancer cells. **a**, Confocal images showing extensive endogenous *S*-nitrosylation (green) in the Golgi apparatus of T-47D cells, shown by colocalization with Golgi marker protein GM-130 (red). Inset shows merged images in higher magnification.

Representative images are shown from a total of three independent experiments. **b**, Pharmacological scavenging of NO in T-47D cells using **methylene blue (MB)** leads to Golgi fragmentation. Fragmented Golgi is observed as a highly vesicular structure (green, Giantin) in methylene blue-treated cells compared to that of the control (DMSO). Representative images are shown from a total of three independent experiments. **c**, Quantification of percentage of cells with fragmented Golgi on treatment with indicated small molecules. Hoechst was used as nuclear stain (blue). Hb, hemoglobin. Scale bar, 10 μ m. Error bars represent standard error of mean (s.e.m.) from three independent experiments. **d**, Proposed model depicting the mechanism responsible for NO scavenging-mediated Golgi fragmentation. NOS3 activity can *S*-nitrosylate cSrc, increasing its activity. Active cSrc can reduce polymerization of actin filaments, resulting in less tensile force and hence intact Golgi. When NOS3 is blocked, cSrc activity is lower, which promotes actin polymerization, thus increasing tensile force and eventual Golgi fragmentation.